Chapter 7

Ultrasound detection of posterior fossa abnormalities in full-term neonates

Sylke J. Steggerda
Francisca T. de Bruïne
Vivianne E.H.J. Smits-Wintjens
Frans J. Walther
Gerda van Wezel-Meijler

Early Human Development 2012; 88:233-239

Abstract

Routine cranial ultrasonography, using the anterior fontanelle as acoustic window enables visualization of the supratentorial brain structures in neonates and young infants. The mastoid fontanelle enables a better view of the infratentorial structures, especially cerebellar hemorrhage in preterm infants. Reports on the usefulness and reliability of cranial ultrasonography using the mastoid fontanelle approach for the detection of posterior fossa abnormalities, focusing only on full-term neonates are limited.

This article describes the technique of mastoid fontanelle ultrasonography in full-term neonates and the features of posterior fossa abnormalities that may be encountered in various neonatal disorders and conditions, combined with subsequent MRI in the same patients. Cranial ultrasound through the mastoid fontanelle plays a pivotal role in the early detection of posterior fossa pathology and selection of neonates with an indication for MRI.

Introduction

Cranial ultrasonography (CUS) is a reliable and non-invasive tool for brain imaging during the neonatal period. It can be performed at the bedside and instantly provides useful diagnostic information to the clinician. It is traditionally performed through the anterior fontanelle (AF). This approach provides a good view of supratentorial structures, but visualization of infratentorial structures is suboptimal because of the distance from the transducer to the posterior fossa (PF). In addition, the echogenic tentorium and vermis impede the detection of lesions (1). By using the mastoid fontanelle (MF) as an additional acoustic window, the transducer is positioned closer to the PF structures and approaches them at a different angle, avoiding the echogenic tentorium. Previous studies have stressed the advantages of CUS using the mastoid fontanelle approach (MF-CUS) for the detection of PF lesions in neonates (2-6). Acquired lesions related to hemorrhage, infarction and infection are mostly described in preterm infants (3,4,6-9), while reports on the applicability of MF-CUS for the detection of PF abnormalities, focusing on full-term neonates are limited.

The more widespread use of magnetic resonance imaging (MRI) has led to an increased detection of cerebellar injury in the high risk full-term neonate. Especially larger cerebellar lesions are associated with a broad spectrum of neurodevelopmental disabilities (10-12).

The aim of this paper is to describe CUS abnormalities of the PF in full-term neonates that may be encountered in various neonatal disorders and conditions such as hypoxic-ischemic encephalopathy (HIE), central nervous system (CNS) infections, intracranial hemorrhage, inborn errors of metabolism and congenital PF malformations. This is illustrated in several cases, showing the characteristics as seen on MF-CUS and MRI. The applicability and the pitfalls and limitations of the MF approach are discussed.

Imaging the posterior fossa: technical aspects

CUS procedure

Cerebellar injury can occur in several conditions, including HIE, CNS infections, traumatic delivery, supratentorial hemorrhage, and inborn errors of metabolism (4,10-12). In these conditions MF-CUS may be helpful for the detection of PF abnormalities. In addition, congenital malformations of the PF may be better depicted when the MF is used (4,11). A high resolution, real-time, 2D ultrasound machine with special settings for the newborn infants' brain and with a multifrequency transducer or different frequency transducers (5, 7.5, 10 MHz) should be used. The transducer should be small enough to fit the MF window (1,5).

The technique of MF-CUS has previously been described in detail (1,4,5). The MF is located at the junction of the posterior parietal, temporal and occipital bones (3). The infant is positioned with the head to one side, and the transducer is placed over the MF, behind the helix of the ear, just above the tragus. The transducer is then slightly moved and rotated until an appropriate view of the PF is obtained. Images can be performed in axial and coronal orientations, from superior to inferior, and provide detailed visualization of the cerebellum (vermis and hemispheres), fourth ventricle, aqueduct and cisterna magna. Figure 1 shows examples of normal CUS images in axial and coronal planes, obtained through the MF in a full-term neonate.

MRI procedure

MRI should be performed in all neonates with clinical or CUS suspicion of parenchymal brain abnormalities. Technical aspects, scanning protocols, and sequences used in neonates have been reported (13). The MRI protocol used for the images in this paper includes T1-weighted three-dimensional turbo field-echo and T2-weighted turbo spin-echo, T2* fast field-echo, and diffusion-weighted imaging (DWI sequences in transverse planes. Slice thickness is 1mm for the T1-weighted images and 2mm for the T2-weighted images without an interslice gap and with a field of view 180-230 mm. The T2* images are especially useful for the detection of micro bleeds in the cerebellum (7).

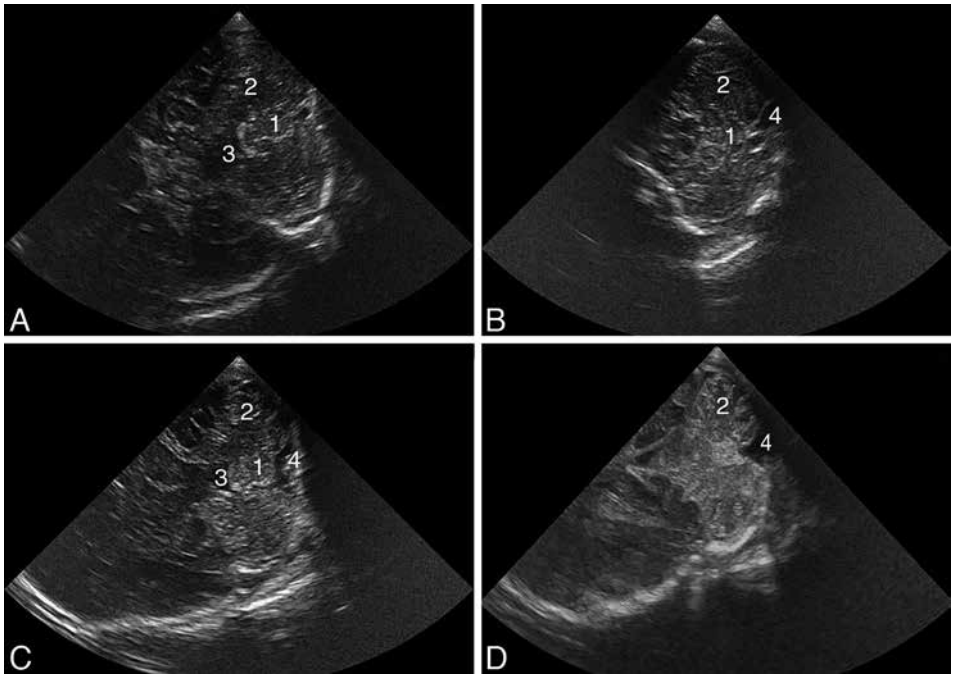

Figure 1. Normal ultrasound scan in full-term neonate using the MF as acoustic window.
Axial views, with **(A)** middle and **(B)** inferior view.
Coronal views with **(C)** middle and **(D)** posterior-inferior view.
Vermis (1), cerebellar hemisphere (the hemisphere located closest to the transducer is visualized in the upper part of the image) (2), fourth ventricle (3), cisterna magna (4).
Note the subtle differences in echogenicity and anatomical details between the two hemispheres, due to differences in distance from the transducer.

Posterior fossa abnormalities in full-term neonates

Hypoxic-ischemic encephalopathy

Although several authors have described a relative sparing of the cerebellum in (near) term neonates with HIE (14,15), the cerebellum can be involved in hypoxic-ischemic neuronal injury with the Purkinje cells and the granule cell neurons being the most vulnerable in the full-term neonate (16,17). Especially the cerebellar vermis is susceptible to injury and a subsequent disturbance of growth has been described (18-20). It is not clear whether this is the result of lesions in the cerebellum that were primary undetected or whether it represents secondary atrophy or degeneration related to

supratentorial brain damage. Primary cerebellar injury has been demonstrated in post-mortem studies (21).

Using MF-CUS, hypoxic-ischemic injury to the cerebellum may be difficult to visualize. Increased echogenicity of the cerebellar vermis and/or hemispheres and loss of foliation can be seen in cases with ischemic injury and edema (Figure 2). In neonates with HIE hemorrhagic injury is also common and both extra axial and parenchymal cerebellar hemorrhage may be encountered, especially after traumatic delivery (11) (Figure 2).

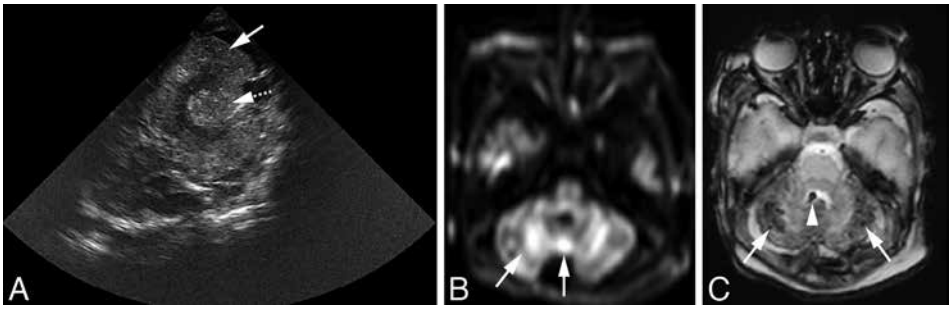

Figure 2. (A) Axial ultrasound scan in full-term neonate (gestational age 37 weeks, severe HIE) performed on 2nd day of life, using the MF as acoustic window, demonstrating abnormal echogenicity of the cerebellar vermis (dotted arrow) and both cerebellar hemispheres (arrow).
(B) and **(C)** MRI in same neonate on 3rd day of life showing a combination of ischemic and hemorrhagic injury. Diffusion-weighted imaging (B) showing abnormal signal intensity in cerebellar vermis and hemispheres (arrows). T_2* FFE scan (C) showing multiple small hemorrhages in both hemispheres (arrows) and in the fourth ventricle (arrowhead).

Central nervous system infection

The neuropathological features of neonatal bacterial meningitis include arachnoiditis, ventriculitis, vasculitis, edema and infarction. This may lead to impaired cerebrospinal fluid (CSF) flow and parenchymal injury, both supra- and infratentorally (17). Systemic fungal or bacterial infections can be complicated by brain abscesses, in both preterm and full-term neonates. Lesions are usually located supratentorially, in the cerebral hemispheres, but can also occur in the cerebellum (4,22,23). Early detection and appropriate treatment are essential. The cerebellum can also be affected in viral infections such as herpes meningoencephalitis (24). In neonates with congenital cytomegalovirus infection, cerebellar hypoplasia may occur (25,26).

On MF-CUS parenchymal injury in CNS infection may appear as focal or diffuse loss of foliation and increased echogenicity of the cerebellar vermis and/ or hemispheres. This may progress to destruction and atrophy of cerebellar structures on follow-up ultrasound scans (Figure 3). Impaired CSF flow may lead to hydrocephalus with a dilated or isolated fourth ventricle. MF-CUS can help identifying the cause and location of the obstruction. Most cases of cerebellar abscesses have been studied by CT or MRI, but they can also be detected by CUS, in particular when scanning is done through the MF (4). Small abscesses can appear as focal, circumscribed echodensities. Larger abscesses may show as echolucent lesions, mostly with an echogenic rim.

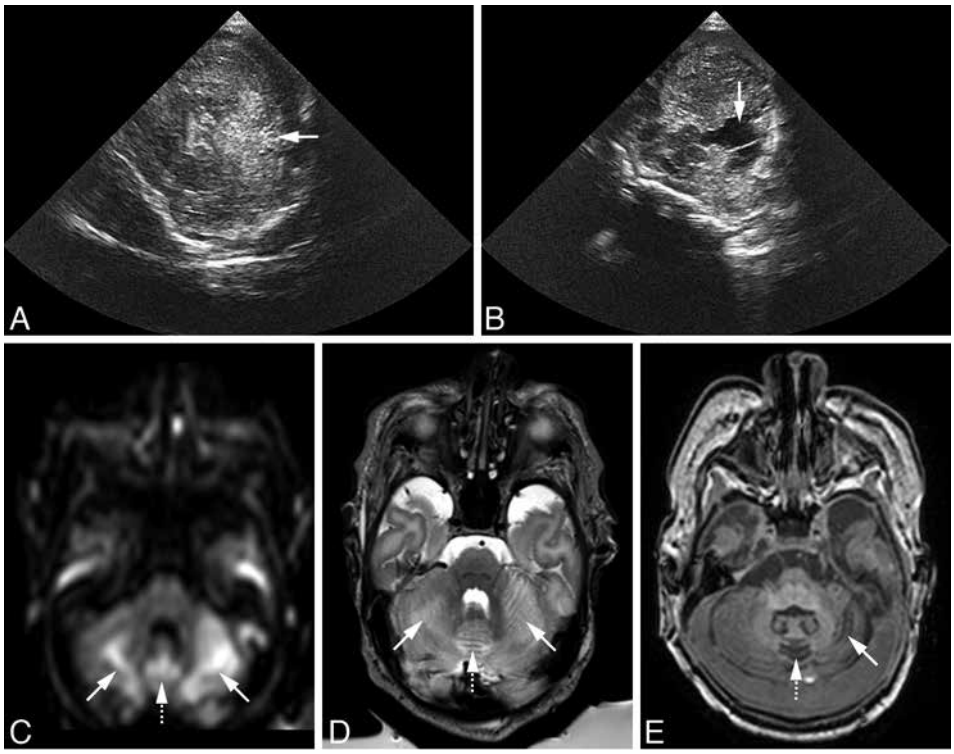

Figure 3. Axial ultrasound scan in full-term neonate (gestational age 40 weeks, Group B streptococcus meningitis) using the right MF as acoustic window. **(A)** On the 4th day of life, demonstrating abnormal echogenicity of cerebellar vermis and hemispheres (arrow). **(B)** Follow-up ultrasound scan on 11th day of life, demonstrating loss of parenchymal tissue of cerebellar vermis and left cerebellar hemisphere and loss of normal structure and anatomical landmarks (arrow).

MRI in same neonate on 5th day of life. **(C)** Diffusion weighted image showing abnormal signal intensity in cerebellar vermis (dotted arrow) and both hemispheres (arrows). **(D)** T2-weighted MRI showing abnormal high signal in corresponding areas (arrows). **(E)** T1-weighted MRI on 12th day of life showing destructive lesions of cerebellar vermis (dotted arrow) and left hemisphere (arrow).

Posterior fossa hemorrhage

Cerebellar hemorrhage can occur in full-term neonates, especially after traumatic delivery, in HIE and in neonates on extracorporeal membrane oxygenation. It is associated with supratentorial hemorrhage, but can also be an isolated finding (10-12). Supratentorial intraventricular hemorrhage is usually easily visible using the AF, but hemorrhage extending into the fourth ventricle, and cerebellar and extra axial PF hemorrhage are more difficult to detect with this approach. The MF enables better and earlier detection of hemorrhage in these structures.

Abnormalities seen on MF-CUS include uni- or bilateral echogenic lesions in the cerebellar vermis and/or hemispheres, echogenicity representing a clot in the fourth ventricle or cisterna magna, thickening of the tentorium and/or peri-mesencephalic cisterns indicating subarachnoid blood, and extra axial blood surrounding the cerebellar hemispheres (Figure 4).

Early detection of PF hemorrhage is of clinical importance, as these neonates are at increased risk of developing post hemorrhagic ventricular dilatation, requiring intensive serial CUS examinations and possibly treatment (27;28). In addition, cerebellar hemorrhage can have major impact on neurodevelopmental outcome, not only in preterm, but also in full-term neonates (10,12).

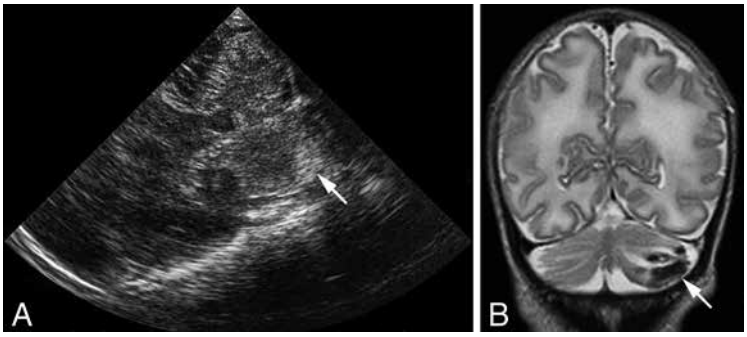

Figure 4. Term neonate (gestational age 40 weeks) born after emergency caesarean section performed for fetal distress, with good Apgar scores. On the 2nd day of life CUS was performed because he was hypertonic and irritable. Conventional CUS using the AF revealed no abnormalities.
(A) Coronal CUS using the right MF as acoustic window demonstrates an echogenic lesion in the left hemisphere, suspect for hemorrhage (arrow). **(B)** Coronal T2-weighted MRI in the same neonate confirms the hemorrhage in the left cerebellar hemisphere (arrow).

Inborn errors of metabolism

Several inborn errors of metabolism can affect the development of the cerebellum during early and late pregnancy (29). Early influence of metabolic disorders on the developing cerebellum can lead to structural abnormalities and hypoplasia, for example in adenylsuccinate lyase deficiency, Zellweger syndrome, pyruvate dehydrogenase complex deficiency, and other mitochondrial diseases (29,30). Other disorders can induce cerebellar atrophy which can be progressive during the first few years of life. In the newborn period this is most frequently and profoundly seen in newborns with carbohydrate deficient glycoprotein syndrome (31-33).

Cerebellar hypoplasia and atrophy can be easily recognized using MF-CUS (Figure 5), although it may be difficult to differentiate between hypoplasia and atrophy of prenatal onset. Measurement of the transcerebellar diameter can be helpful to assess whether cerebellar size is appropriate for gestational age (34,35) (Figure 5). Cerebellar hypoplasia and atrophy are non specific findings. Combined with a clinical picture suggesting a metabolic disorder, these abnormalities can help diagnosing the underlying disease.

Congenital posterior fossa malformations

MF-CUS is a valuable tool for imaging of congenital PF anomalies. Abnormal fluid collections, such as a retrocerebellar arachnoid cyst and mega cisterna magna, can be visualized (Figure 5). An arachnoid cyst is a pocket of CSF without communication with the fourth ventricle, which can cause mass effect on the adjacent cerebellar parenchyma. Mega cisterna magna is an increased retrocerebellar CSF space, the vermis and cerebellar hemispheres are generally normal (36).

Focal hypoplasia of the cerebellar vermis or one of the cerebellar hemispheres and generalized hypoplasia can be detected. Cerebellar hypoplasia may be isolated or associated with syndromic disorders. It can occur in combination with corpus callosum agenesis, a hypoplastic pons (in pontocerebellar hypoplasia) or cystic PF malformation (as part of the Dandy Walker continuum). The classic Dandy Walker malformation is characterized by a hypoplastic cerebellar vermis that is rotated upwards, cystic dilatation of the fourth ventricle and enlargement of the posterior fossa with elevated tentorium (Figure 6) (36,37).

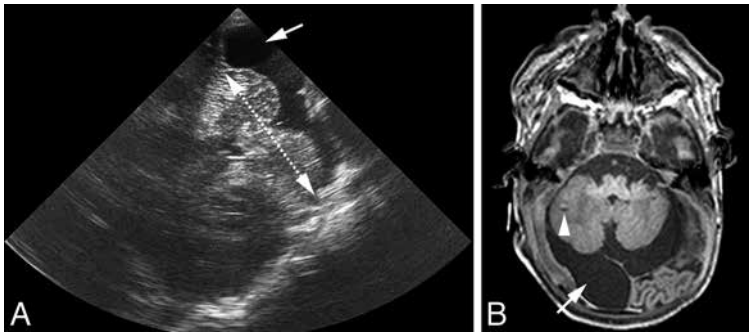

Figure 5. Term neonate (gestational age 40 weeks) with pyruvate dehydrogenase complex deficiency. Conventional CUS using the AF showed large bilateral germinolytic cysts (not shown).
(A) CUS using right MF as acoustic window demonstrates cerebellar hypoplasia with small transcerebellar diameter of 45 mm and a possible cyst in the PF (arrow). **(B)** T1-weighted MRI in same neonate demonstrating cerebellar hypoplasia and an arachnoid cyst (arrow). In addition, a small punctate hemorrhage was seen in the right cerebellar hemisphere (arrowhead), not detected by CUS.

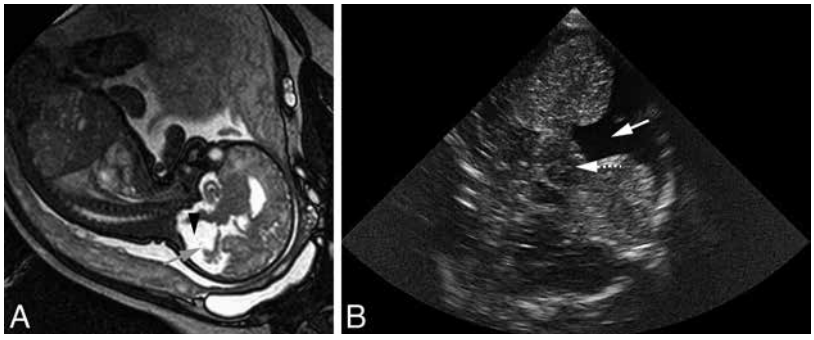

Figure 6. (A) Fetal MRI (gestational age 35 weeks) in neonate with PF malformation. Sagittal T2-weighted image shows a Dandy Walker malformation with an enlarged PF, a dilated fourth ventricle (arrowhead) and a hypoplastic, upward rotated vermis (arrow). **(B)** Postnatal axial CUS using the MF showing an enlarged PF and dilated, trapezoid shaped fourth ventricle (arrow) communicating with a retrocerebellar cyst. The vermis could not be detected. Dotted arrow indicates the pons, located anterior to the fourth ventricle.

Measurement of the transcerebellar diameter

The transcerebellar diameter can be measured accurately using the MF (Figure 5). A good correlation between transcerebellar diameter and gestational age has been described both in appropriate and small for gestational age neonates, and normal values are available (34,38). In infants with an accurate determination of gestational age a reduced transcerebellar diameter at birth may indicate congenital cerebellar hypoplasia. This is often associated with structural CNS malformations, chromosomal disorders, congenital cytomegalovirus infection and inborn errors of metabolism. It may also reflect atrophy due to an insult causing direct cerebellar injury or may result from crossed cerebellar atrophy as can occur in cases with large supratentorial lesions (34,39).

Pitfalls and limitations

When looking for PF malformations, one should be aware of a pitfall of MF-CUS. In the most posterior coronal plane a communication between the fourth ventricle and the cisterna magna via the foramen of Magendie may be seen. This can give a false impression of inferior vermian agenesis (2,3). Imaging at different angles in axial and coronal planes through the MF, in combination with a good quality midline sagittal image obtained through the AF or posterior fontanelle, is usually sufficient to prevent an erroneous diagnosis of vermian agenesis.

As in conventional CUS using the AF, there are limitations of MF-CUS. First of all it is operator dependent. Adding MF-CUS as a routine while performing CUS examinations, will increase experience and expertise of the sonographist. This enables recognition of the normal appearance and anatomy of the PF and of scanning artifacts, and improves the detection rate of PF abnormalities.

Scanning artifacts are not uncommon and may lead to misinterpretation and/or false diagnoses, especially in infants at risk of PF abnormalities. Imaging in both axial and coronal orientations and scanning through both mastoid fontanels can help distinguishing artifacts from focal lesions.

Furthermore, image quality may be affected by the small size of the MF. The near field and nearest cerebellar hemisphere are generally better depicted than the hemisphere that is farthest away from the transducer. The echogenicity of the cerebellar hemispheres may seem asymmetric depending on the angulation of and distance to the transducer (Figure 1). In these cases the use of both mastoid fontanels will improve the performance of MF-CUS.

Discussion

MF-CUS is a valuable tool for the detection of cerebellar injury in preterm infants. It is also useful in the full-term newborn with PF abnormalities, not only for the detection of hemorrhage and congenital malformations but also in cases with (suspected) HIE, CNS infections and inborn errors of metabolism. The major advantages of MF-CUS in full-term neonates at risk of PF abnormalities are that it is safe, can be performed at the bedside and instantly provides diagnostic information, enabling early detection and diagnosis before MRI is feasible in sick, instable neonates. For an experienced sonographer it requires only a few minutes of additional scanning time to obtain the images.

However, there are also limitations of MF-CUS. Smaller lesions may be missed and false positive diagnoses may occur. Therefore, additional MRI is necessary in neonates with (suspected) PF abnormalities. MRI enables detailed visualization of the whole brain, showing the exact location and extent of abnormalities, and it may provide additional information on the underlying cause. However, it is a more burdening procedure requiring transportation of the neonate to the MRI unit and, in some cases, sedation. This makes MRI less suitable for early detection and undesirable for serial imaging.

In conclusion, (serial) MF-CUS is a useful technique to detect PF abnormalities in the full-term neonate. MRI is needed to confirm the diagnosis, to detect smaller lesions and to avoid false positive diagnoses.
Studies comparing MF-CUS with MRI are necessary to investigate the reliability of MF-CUS for the detection of PF abnormalities in the full-term neonate.

References

1. van Wezel-Meijler G. Neonatal Cranial Ultrasonography: Guidelines for the Procedure and Atlas of Normal Ultrasound Anatomy. Springer Berlin Heidelberg; 2007.
2. Buckley KM, Taylor GA, Estroff JA, Barnewolt CE, Share JC, Paltiel HJ. Use of the mastoid fontanelle for improved sonographic visualization of the neonatal midbrain and posterior fossa. AJR Am J Roentgenol 1997; 168:1021-1025.
3. Di Salvo DN. A new view of the neonatal brain: clinical utility of supplemental neurologic US imaging windows. Radiographics 2001; 21:943-955.
4. Enriquez G, Correa F, Aso C, et al. Mastoid fontanelle approach for sonographic imaging of the neonatal brain. Pediatr Radiol 2006; 36:532-540.
5. Steggerda SJ, Leijser LM, Walther FJ, van Wezel-Meijler G. Neonatal cranial ultrasonography: how to optimize its performance. Early Hum Dev 2009; 85:93-99.
6. Luna JA, Goldstein RB. Sonographic visualization of neonatal posterior fossa abnormalities through the posterolateral fontanelle. AJR Am J Roentgenol 2000; 174:561-567.
7. Steggerda SJ, Leijser LM, Wiggers-de Bruine FT, Grond van der GJ, Walther FJ, van Wezel-Meijler G. Cerebellar injury in preterm infants: incidence and findings on US and MR images. Radiology 2009; 252:190-199.
8. Limperopoulos C, Benson CB, Bassan H, et al. Cerebellar hemorrhage in the preterm infant: ultrasonographic findings and risk factors. Pediatrics 2005; 116:717-724.
9. Merrill JD, Piecuch RE, Fell SC, Barkovich AJ, Goldstein RB. A new pattern of cerebellar hemorrhages in preterm infants. Pediatrics 1998; 102:E62.
10. Limperopoulos C, Robertson RL, Sullivan NR, Bassan H, du Plessis AJ. Cerebellar injury in term infants: clinical characteristics, magnetic resonance imaging findings, and outcome. Pediatr Neurol 2009; 41:1-8.
11. Miall LS, Cornette LG, Tanner SF, Arthur RJ, Levene MI. Posterior fossa abnormalities seen on magnetic resonance brain imaging in a cohort of newborn infants. J Perinatol 2003; 23:396-403.
12. Williamson WD, Percy AK, Fishman MA, et al. Cerebellar hemorrhage in the term neonate: developmental and neurologic outcome. Pediatr Neurol 1985; 1:356-360.
13. van Wezel-Meijler G, Leijser LM, de Bruine FT, Steggerda SJ, Grond van der GJ, Walther FJ. Magnetic resonance imaging of the brain in newborn infants: practical aspects. Early Hum Dev 2009; 85:85-92.
14. Triulzi F, Parazzini C, Righini A. Patterns of damage in the mature neonatal brain. Pediatr Radiol 2006; 36:608-620.
15. Vermeulen RJ, Fetter WP, Hendrikx L, Van Schie PE, van der Knaap MS, Barkhof F. Diffusion-weighted MRI in severe neonatal hypoxic ischaemia: the white cerebrum. Neuropediatrics 2003; 34:72-76.
16. Lawrence RK, Inder TE. Anatomic changes and imaging in assessing brain injury in the term infant. Clin Perinatol 2008; 35:679-93.
17. Volpe. Neurology of the newborn. (ed. 5). Philadelphia: Saunders. 2008; page 351.
18. Sargent MA, Poskitt KJ, Roland EH, Hill A, Hendson G. Cerebellar vermian atrophy after neonatal hypoxic-ischemic encephalopathy. AJNR Am J Neuroradiol 2004; 25:1008-1015.
19. Connolly DJ, Widjaja E, Griffiths PD. Involvement of the anterior lobe of the cerebellar vermis in perinatal profound hypoxia. AJNR Am J Neuroradiol 2007; 28:16-19.

20. Le Strange E, Saeed N, Cowan FM, Edwards AD, Rutherford MA. MR imaging quantification of cerebellar growth following hypoxic-ischemic injury to the neonatal brain. AJNR Am J Neuroradiol 2004; 25:463-468.
21. Jouvet P, Cowan FM, Cox P, et al. Reproducibility and accuracy of MR imaging of the brain after severe birth asphyxia. AJNR Am J Neuroradiol 1999; 20:1343-1348.
22. Correa F, Enriquez G, Rossello J, et al. Posterior fontanelle sonography: an acoustic window into the neonatal brain. AJNR Am J Neuroradiol 2004; 25:1274-1282.
23. Huang CC, Chen CY, Yang HB, Wang SM, Chang YC, Liu CC. Central nervous system candidiasis in very low-birth-weight premature neonates and infants: US characteristics and histopathologic and MR imaging correlates in five patients. Radiology 1998; 209:49-56.
24. Vossough A, Zimmerman RA, Bilaniuk LT, Schwartz EM. Imaging findings of neonatal herpes simplex virus type 2 encephalitis. Neuroradiology 2008; 50:355-366.
25. de Vries LS, Gunardi H, Barth PG, Bok LA, Verboon-Maciolek MA, Groenendaal F. The spectrum of cranial ultrasound and magnetic resonance imaging abnormalities in congenital cytomegalovirus infection. Neuropediatrics 2004; 35:113-119.
26. Barkovich AJ, Lindan CE. Congenital cytomegalovirus infection of the brain: imaging analysis and embryologic considerations. AJNR Am J Neuroradiol 1994; 15:703-715.
27. Cramer BC, Walsh EA. Cisterna magna clot and subsequent post-hemorrhagic hydrocephalus. Pediatr Radiol 2001; 31:153-159.
28. Taylor GA. Sonographic assessment of posthemorrhagic ventricular dilatation. Radiol Clin North Am 2001; 39:541-551.
29. Steinlin M, Blaser S, Boltshauser E. Cerebellar involvement in metabolic disorders: a pattern-recognition approach. Neuroradiology 1998; 40:347-354.
30. Lindhard A, Graem N, Skovby F, Jeppesen D. Postmortem findings and prenatal diagnosis of Zellweger syndrome. Case report. APMIS 1993; 101:226-228.
31. Jensen PR, Hansen FJ, Skovby F. Cerebellar hypoplasia in children with the carbohydrate-deficient glycoprotein syndrome. Neuroradiology 1995; 37:328-330.
32. Antoun H, Villeneuve N, Gelot A, Panisset S, Adamsbaum C. Cerebellar atrophy: an important feature of carbohydrate deficient glycoprotein syndrome type 1. Pediatr Radiol 1999; 29:194-198.
33. Drouin-Garraud V, Belgrand M, Grunewald S, et al. Neurological presentation of a congenital disorder of glycosylation CDG-Ia: implications for diagnosis and genetic counseling. Am J Med Genet 2001; 101:46-49.
34. Makhoul IR, Goldstein I, Epelman M, Tamir A, Reece EA, Sujov P. Neonatal transverse cerebellar diameter in normal and growth-restricted infants. J Matern Fetal Med 2000; 9:155-160.
35. Davies MW, Swaminathan M, Betheras FR. Measurement of the transverse cerebellar diameter in preterm neonates and its use in assessment of gestational age. Australas Radiol 2001; 45:309-312.
36. Barkovich AJ. Diagnostic imaging pediatric neuroradiology. First edition. Salt Lake City: Amirsys. 2007; page 82-85.
37. Patel S, Barkovich AJ. Analysis and classification of cerebellar malformations. AJNR Am J Neuroradiol 2002; 23:1074-1087.
38. Hagmann CF, Robertson NJ, Acolet D, et al. Cerebral measurements made using cranial ultrasound in term Ugandan newborns. Early Hum Dev 2011; 87:341-347.
39. Gallini F, Luciano R, Pane M, De Carolis MP, Romagnoli C, Mercuri E. Crossed cerebellar atrophy of prenatal onset. Childs Nerv Syst 2006; 22:734-736.